

Local Heat Transfer in Open Frame Cavities of Fenestration Systems

Thomas R. Branchaud

Dragan Curcija, Ph.D.
Member ASHRAE

William P. Goss, Ph.D.
Member ASHRAE

ABSTRACT

The current practice in North America for predicting the overall (convection and radiation) heat transfer in fenestration product frame surface cavities that are open to the outdoor or indoor environment, using fenestration system heat transfer computer models, is specified in draft ASHRAE Standard 142P (1998). For the outdoor side of a fenestration product, it is recommended that the external boundary condition be brought into the cavity a distance equal to five times the width of the exterior opening (the so-called "five-times rule"). On the indoor side, a "one-times" convention is used (one times the width of the cavity opening). These rules or conventions do not appear to be supported by any solid technical data or by any published research. In European practice, upper and lower limits of the heat transfer through closed and partially open frame cavities are currently proposed. In this paper, computer modeling of an aluminum frame window with outdoor frame surface cavities was performed using a finite-element computational fluid dynamics method. The model included turbulent parallel outdoor flow past an aluminum-framed horizontal slider with a profile that included several frame exterior surface cavities. The heat transfer results from this study indicate that significant convective heat transfer effects extend only up to one times the width of the cavity opening. Therefore, it can be concluded that the penetration of forced convective effects in open frame cavities is not the function of the type of airflow (i.e., outdoor forced vs. indoor natural convection). From the results of this study, and also considering the view factors for the radiant heat transfer exchange that occurs in the cavity, it may be concluded that a "one times" convention would be more appropriate for both outdoor (weather) and indoor (room) side surface cavities of fenestration systems.

INTRODUCTION

This paper addresses the turbulent convective heat transfer coefficients on the exterior surfaces of a real window where the flow is parallel to the glass surface of the window. The details of this work can be found in Branchaud (1997). Prior research work for impinging (called "perpendicular") exterior laminar flow conditions is given in Curcija (1992) and Curcija and Goss (1995). Curcija (1992) and Curcija and Goss (1995) give natural (free) convection heat transfer results for flow over interior fenestration surfaces. Curcija (1992) and Curcija and Goss (1994) present two-dimensional analyses of the heat transfer through fenestration products that show how the exterior and interior overall heat transfer coefficients (combined radiation and convection) are used in determining the overall U-factor of fenestration products.

The research reported here focuses on the current practice in North America for predicting the overall (convective and radiative) heat transfer in fenestration product frame surface cavities that are open on vertical and/or horizontal surfaces to the outdoor or indoor environment. Frame surface cavities differ from internal frame cavities in several ways. An exterior frame surface cavity is partially subjected to forced convection and radiant heat transfer to the colder outdoor environment, and an interior frame surface cavity is partially subjected to natural convection and radiant heat transfer from the warmer indoor environment. Internal frame cavities, if properly sealed, experience enclosure natural convective heat transfer and radiant heat transfer to the other surfaces within the cavity. Heat transfer effects of outdoor or indoor environmental conditions would only occur in situations where there is air leakage through the internal frame cavity.

Thomas R. Branchaud is engineering manager at Wakefield Engineering Inc., Beverly, Mass.; Dragan Curcija is president of Carli, Inc., Amherst, Mass.; and William P. Goss is a professor in the Department of Mechanical and Industrial Engineering, University of Massachusetts, Amherst.

For fenestration system heat transfer computer models, the levels of penetration of the outdoor (or indoor) boundary conditions into frame surface cavities are recommended in draft ASHRAE Standard 142P (ASHRAE 1996). For the outdoor side of a fenestration product, it is recommended that "if the cavity that is open to the outdoor side extends more than five times the width of its opening into the frame, the air cavity beyond the five-times width shall be considered as an enclosed air cavity." This is sometimes called the "five-times rule." In this paper we will call it the "five-times convention." On the indoor side, a "one-times convention" is used, which states that "the portion of any cavity greater than one times the cavity width shall be treated as an enclosed air cavity." These conventions do not appear to be supported by any solid technical data or by any published heat transfer research but rather by using trial and error on overall U-factors and ad hoc "educated guess" procedures.

In international practice, prEN ISO/CD 10077-Part 2 (ISO 1998) specifies that grooves and cavities "connected to the exterior or interior by a slit greater than 2 mm but not exceeding 10 mm are to be considered as slightly ventilated air cavities. The equivalent conductivity . . . is twice that of an unventilated air cavity of the same size." For cavities with openings greater than 10 mm, it is assumed that the entire cavity is exposed to the appropriate interior or exterior overall heat transfer coefficient. In the case of a large cavity connected by a single slit and a developed surface exceeding the width of the slit by a factor of 10, the surface resistance with reduced radiation should be used. To the authors' knowledge, there does not appear to be any technical basis for any of these conventions, and they may be changed in the final draft of the CEN/ISO document.

MATHEMATICAL FORMULATION

Turbulent, forced convection can be described by the conservation of mass, Newton's second law (momentum), and the conservation of energy in two-dimensional partial differential equation form. The two-equation, k - ϵ turbulence model was used in the turbulent, forced convection calculations, which adds two transport equations—kinetic energy and dissipation (Launder and Spalding 1972). Several assumptions and approximations are made prior to the solution of this set of equations:

- The air is assumed to be an ideal gas and an incompressible fluid.
- The dynamic viscosity is assumed constant.
- The momentum and energy equations are weakly coupled (momentum is not temperature dependent).
- The flow is two-dimensional.
- The flow is steady state.
- The dissipation function in the energy equation is negligible.

The equations can be written in nondimensional form by using the following scaling:

$$x^\circ = \frac{x}{L}; u^\circ = \frac{u}{U}; p^\circ = \frac{\mu}{\rho^2 U^3 L} p;$$

$$T^\circ = \frac{T - T_{fluid}}{\Delta T}; k^\circ = \frac{k}{U^2}; \epsilon^\circ = \frac{\epsilon L}{U^3}$$

where L , U , and ΔT are the characteristic length, velocity, and temperature difference.

The resulting set of partial differential equations that govern the turbulent forced convection in two dimensions are, in nondimensional form:

Continuity:

$$\frac{\partial u^\circ}{\partial x^\circ} + \frac{\partial v^\circ}{\partial y^\circ} = 0$$

Momentum:

$$u^\circ \frac{\partial u^\circ}{\partial x^\circ} + v^\circ \frac{\partial u^\circ}{\partial y^\circ} = -\frac{\partial p^\circ}{\partial x^\circ} + \frac{1}{\text{Re}}$$

$$\mu^\circ \left(\frac{\partial^2 u^\circ}{\partial x^{\circ 2}} + \frac{\partial^2 u^\circ}{\partial y^{\circ 2}} \right) + 2 \frac{\partial \mu^\circ}{\partial x^\circ} \frac{\partial u^\circ}{\partial x^\circ} + \frac{\partial \mu^\circ}{\partial x^\circ} \left(\frac{\partial u^\circ}{\partial y^\circ} + \frac{\partial v^\circ}{\partial x^\circ} \right)$$

$$u^\circ \frac{\partial v^\circ}{\partial x^\circ} + v^\circ \frac{\partial v^\circ}{\partial y^\circ} = -\frac{\partial p^\circ}{\partial y^\circ} + \frac{1}{\text{Re}}$$

$$\mu^\circ \left(\frac{\partial^2 v^\circ}{\partial x^{\circ 2}} + \frac{\partial^2 v^\circ}{\partial y^{\circ 2}} \right) + 2 \frac{\partial \mu^\circ}{\partial y^\circ} \frac{\partial v^\circ}{\partial y^\circ} + \frac{\partial \mu^\circ}{\partial y^\circ} \left(\frac{\partial u^\circ}{\partial y^\circ} + \frac{\partial v^\circ}{\partial x^\circ} \right)$$

Energy:

$$u^\circ \frac{\partial T^\circ}{\partial x^\circ} + v^\circ \frac{\partial T^\circ}{\partial y^\circ} = \frac{1}{\text{Pe}}$$

$$\frac{\partial \lambda^\circ}{\partial x^\circ} \frac{\partial T^\circ}{\partial x^\circ} + \frac{\partial \lambda^\circ}{\partial y^\circ} \frac{\partial T^\circ}{\partial y^\circ} + \lambda^\circ \left(\frac{\partial^2 T^\circ}{\partial x^{\circ 2}} + \frac{\partial^2 T^\circ}{\partial y^{\circ 2}} \right)$$

Turbulent kinetic energy:

$$u^\circ \frac{\partial k^\circ}{\partial x^\circ} + v^\circ \frac{\partial k^\circ}{\partial y^\circ} = \frac{1}{\sigma_k} \left(\frac{\partial \mu_r^\circ}{\partial x^\circ} \frac{\partial k^\circ}{\partial x^\circ} + \frac{\partial \mu_r^\circ}{\partial y^\circ} \frac{\partial k^\circ}{\partial y^\circ} \right) + \frac{\mu_r^\circ}{\sigma_k} \left(\frac{\partial^2 k^\circ}{\partial x^{\circ 2}} + \frac{\partial^2 k^\circ}{\partial y^{\circ 2}} \right) - \rho \epsilon^\circ$$

Turbulent dissipation:

$$u^\circ \frac{\partial \epsilon^\circ}{\partial x^\circ} + v^\circ \frac{\partial \epsilon^\circ}{\partial y^\circ} = \frac{1}{\sigma_\epsilon} \left(\frac{\partial \mu_e^\circ}{\partial x^\circ} \frac{\partial \epsilon^\circ}{\partial x^\circ} + \frac{\partial \mu_e^\circ}{\partial y^\circ} \frac{\partial \epsilon^\circ}{\partial y^\circ} \right) + \frac{\mu_e^\circ}{\sigma_\epsilon} \left(\frac{\partial^2 \epsilon^\circ}{\partial x^{\circ 2}} + \frac{\partial^2 \epsilon^\circ}{\partial y^{\circ 2}} \right) - \rho c_2 \frac{\epsilon^{\circ 2}}{k^\circ}$$

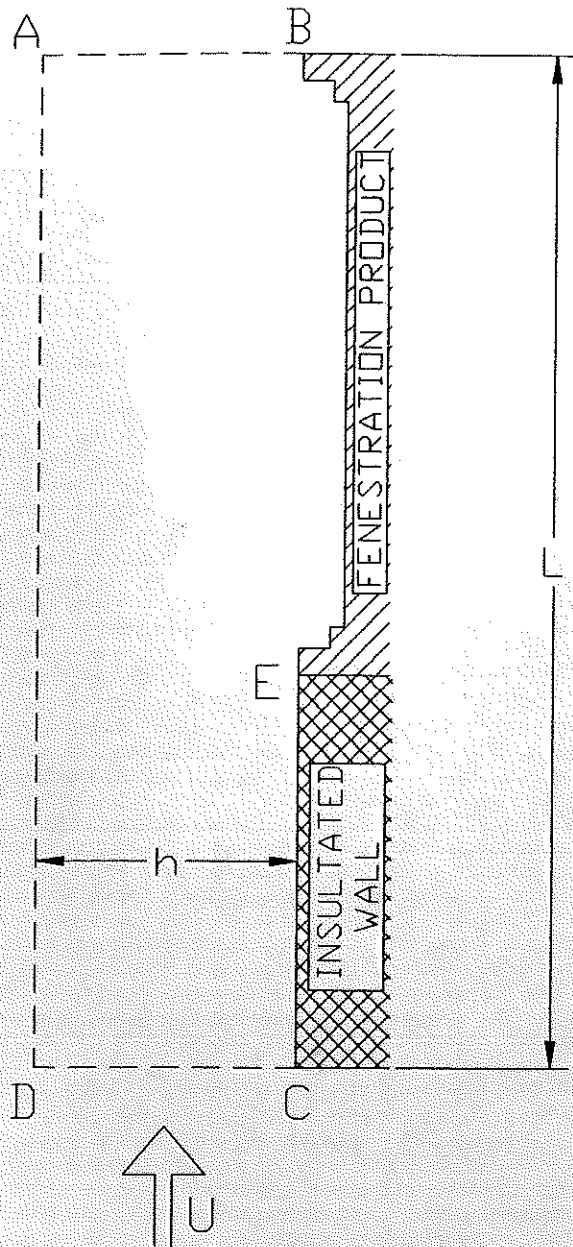


Figure 1 Domain on which the governing equations are solved.

Figure 1 shows a schematic of the fluid flow domain (A-B-E-C-D) adjacent to a fenestration product (window) and an insulated wall (surround panel). The following boundary conditions were used in the finite-element calculations of turbulent forced convection over the surface of the surround panel and window:

- C-E (surround panel): $u = v = dT/dy = 0$
no k or ϵ B.C.'s at wall
- E-B (window surface): $u = v = 0, T = 21^\circ\text{C}$
no k or ϵ B.C.'s at wall

- C-D (inlet): $u = 6.7 \text{ m/s}, v = 0, T = -17.8^\circ\text{C}$
 $k = 1.5 I (6.7 \text{ m/s})^2, \epsilon = \rho c_\mu k^2 / r_\mu \mu$
($I = \text{turbulent intensity} = 3.5\%$,
 $c_\mu = 0.9, R_\mu = 100$)
- D-A and A-B
($y = \infty$ and outlet): $\tau = dT/dy = dk/dy = d\epsilon/dy = 0$

The numerical technique used to solve the above system of partial differential equations was the finite-element method (FEM), which discretizes the solution domain into elements and applies the governing partial differential equations in a residual form to each element. The differential equations can then be written as a system of algebraic equations for each element, and thus a global system of algebraic equations can be assembled using the connectivity of the elements (elements share nodal points). The system of algebraic equations is organized into matrix form, and the solution of the global matrix equation is iterative due to the nonlinearity of the momentum equations. Details regarding the assembly of the matrix equations used in the numerical technique can be found in FDI (1993). A good source for general finite-element theory is Burnett (1987), while Baker (1983) reviews the application of FEM to fluid flow and heat transfer problems.

The k - ϵ model is based on high Reynolds number flow (Launder and Spalding 1972) and therefore is not valid in the near-wall viscous sublayer due to the low Reynolds number flow there (the flow in the sublayer nearest the wall is laminar). FDI (1993) uses special wall elements having shape functions that mimic the universal law of the wall velocity and temperature profiles. The k and ϵ turbulent transport equations are not solved in the near-wall region; instead, the distribution of the turbulent diffusivities of momentum and heat are based upon van Driest's mixing length model (Holman 1990).

Semi-empirical approximations of the profiles of the nondimensional velocity u^+ and temperature T^+ near the wall have been developed based on empirical data. The wall element shape functions for velocity and temperature in the direction normal to the wall are based on these approximations, while the shape functions in the direction parallel to the wall are the functions used in the remainder of the domain. Detailed information regarding these elements can be found in FDI (1993).

VALIDATION OF NUMERICAL TECHNIQUE

Outdoor airflow over a fenestration system results in a complicated flow pattern that is different for each fenestration product. The results of the fenestration, finite-element heat transfer model cannot be compared to currently published overall experimental results, which have little or no two-dimensional detail, for purposes of validation. Turbulent convective flow over a fenestration system exhibits both boundary layer flows and separated flow regions (due to the frame obstructions). Calculations for each of these flow conditions (for which there are published results for comparison)

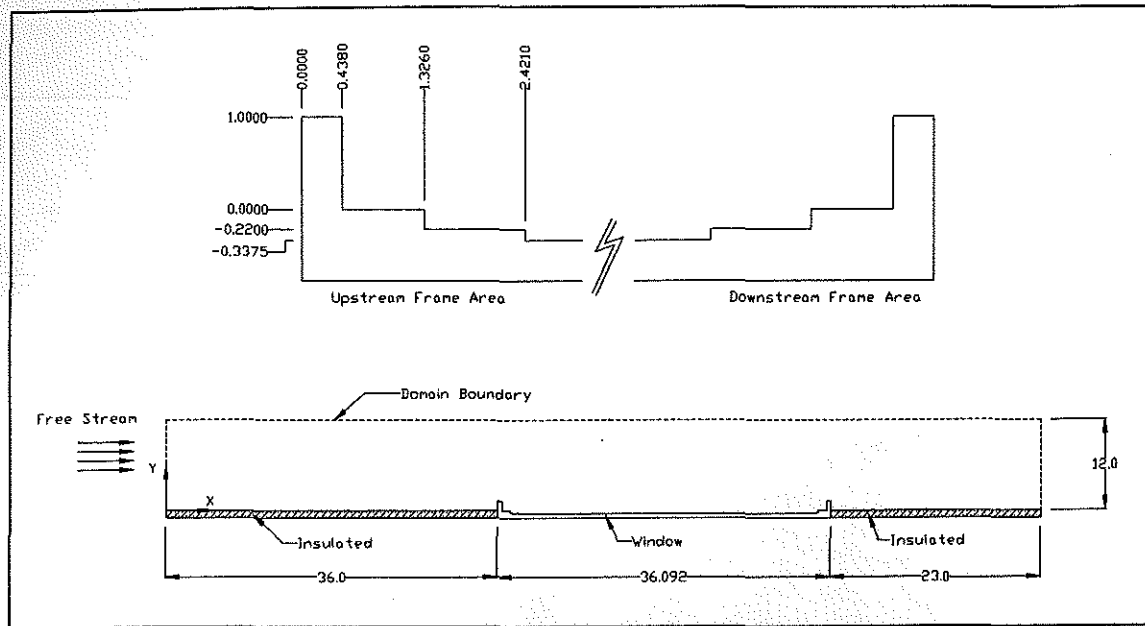


Figure 2a Sketch of solution for "slider side" idealized surface calculations; sketch of system, dimensions in inches.

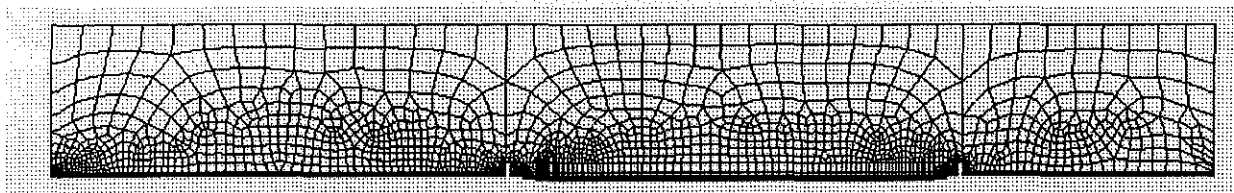


Figure 2b Sketch of solution for "slider side" idealized surface calculation; finite element mesh.

were performed. Branchaud (1997) presents validation results for turbulent boundary layer type flow over a flat plate and for turbulent separated flows downstream of a backward-facing step, both of which are typical surfaces in window frame profiles. The finite-element calculated results showed very good agreement to previously published, generally accepted experimental results. This validated the finite-element solution technique used in this paper for analyzing turbulent flow along the exterior surface of a fenestration product with separation and reattachment regions.

AIRFLOW OVER THE FENESTRATION SYSTEM

The fenestration system chosen for this study was an aluminum horizontal sliding window. The window has two sides, referred to as the *slider side* and the *stationary side*, having different surface geometries exposed to the outdoor conditions. The slider side moves on rollers in the horizontal direction behind the stationary side, such that the stationary side remains exposed to the outdoor environment. To keep the length of this paper reasonable, only a portion of the more geometrically complex slider side results will be presented.

Details of the stationary side analyses may be found in Branchaud (1997). Figure 2a presents a schematic of the slider side calculation domain, and Figure 2b gives the finite-element mesh used. The geometry of the slider side has been simplified somewhat to reduce the complexity of the supercomputer calculations. The flow recirculation around the upstream and downstream frame obstructions and steps required a high concentration of nodes to resolve the high gradients of velocity in these regions.

The nondimensional loading parameters, $Re = 1.2765 \times 10^4$ and $Pe = 9.14 \times 10^3$, were calculated using a characteristic length, L , of 0.0254 m (1 in., the height of the frame obstruction), and a characteristic velocity, U , of 6.7 m/s (15 mph). The assumed free-stream turbulent intensity, I , of 3.5% yields nondimensional values of the kinetic energy and dissipation on the inlet boundary of $k^o = 0.001838$ and $\epsilon^o = 0.0003882$.

Figure 3 shows the velocity fields in the regions near the upstream (sill) and downstream (head) frame sections. The frame obstructions cause low-speed circulating flow regions at each abrupt change in geometry. The two backward-facing steps just downstream of the first frame obstruction delay the reattachment of the flow to the downstream flat-plate window glass surface (insulated glazing unit, or IGU). However, reat-

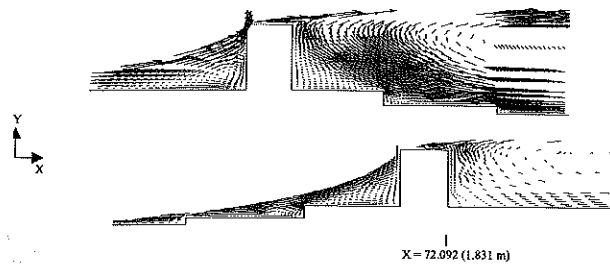


Figure 3 Velocity vector plots of regions near upstream frame (sill) and downstream frame (head), for slider side calculations.

tachment occurs along the glass surface for both the slider side and protrusion calculations, and flat-plate velocity and temperature profiles exist before the downstream frame or protrusion. The relative sizes of the velocity vectors illustrate the low-speed recirculating flow in the immediate area of the frame geometry changes.

HEAT TRANSFER RESULTS

A finite-element calculation that included all of the slider side frame details resulted in a very high number of nodal points and could not be solved due to limitations of the available computer resources. Therefore, two separate calculations with different geometric simplifications were used. Each gave detailed heat transfer information about different surfaces of the actual geometry. In the first calculations (referred to as the "slider side" calculations), the frame details were rectangular shapes without any frame cavities in the two protruding obstructions. The second set of calculations (called "protrusion detail" calculations) used the actual geometry for the horizontal surface obstructions with the frame cavities included and eliminated the subsequent steps in the frame geometry. Figure 4 gives the exterior geometries used in the slider side and protrusion detail calculations. Only the local convective heat transfer coefficient results of the protrusion detail calculations are presented in this paper.

Figure 5a gives the protrusion detail calculation results for the local heat transfer coefficient on the "sheltered" surfaces in the actual upstream frame surfaces of the initial upstream obstruction. Figure 5b gives the protrusion detail calculation results for the local heat transfer coefficient on the sheltered surfaces in the actual downstream frame surfaces of the downstream obstruction. The unsheltered surfaces of these two obstructions had already been considered in the slider side calculations and are documented in Branchaud (1997). The sheltered surfaces of the upstream obstruction are exposed to very low air velocities, and, as a result, the value of the local heat transfer coefficient is low (approaching the conduction limit) as the recirculating pocket of air acts as an insulating region. There is a slight recirculation region in the cavity of the downstream frame obstruction, and, as a result, the values of h on the inside cavity walls are near zero at the bottom of the cavity and increase to a relatively low value near the top. The

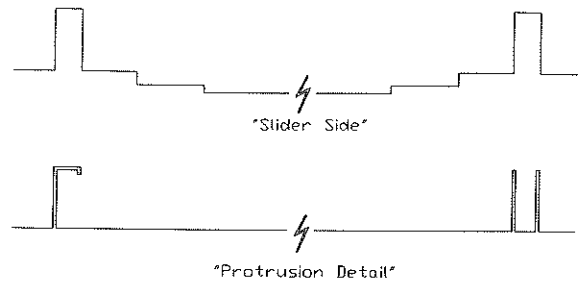


Figure 4 Comparison of "slider side" to "protrusion detail" models.

heat transfer effects in this cavity extend into the cavity about one times the width of the cavity in contrast to the often used approximations of five times the cavity width (the so-called five-times rule). Similar results might be expected for an impinging (erroneously called perpendicular) flow. For impinging flows, only the initial flow is perpendicular to the fenestration product glass surface, since the flow turns parallel in the vicinity of the fenestration product surfaces and is essentially parallel at the upper and lower frame surfaces (Curcija and Goss 1995).

CONCLUSIONS AND RECOMMENDATIONS

Parallel flow over a fenestration system under standard ASHRAE (1996, 1997) winter conditions of -17.8°C (0°F) outside air temperature and 6.7 m/s (15 mph) outside free-stream wind speed for a normal size window with frames that protrude into the airstream is most likely turbulent. Laminar convective heat transfer models of these windows did not converge at velocities significantly lower than the assumed wind speed.

Separation and recirculation in regions of frame geometry changes result in slow-moving, circulating, warmer pockets of air. These regions of separation and recirculation have relatively lower values of the heat transfer coefficient. They effectively act as insulating layers on the outside fenestration system surfaces, thus inhibiting local convective heat transfer. This nonuniform distribution of the heat transfer coefficient on the outdoor surface may act to lower the overall heat transferred through a fenestration system.

The turbulent flow heat transfer model used in this study included turbulent airflow past an aluminum horizontal slider window profile. The heat transfer results indicate that significant convective heat transfer effects extend only up to one times the width of the cavity opening for the case studied in this paper. This is in contrast to the previously accepted approximation of five times the width of the cavity opening.

This study has shown that there can be a significant variation of the local convective heat transfer coefficient on the outdoor surface of a fenestration system (depending on its geometry). It is recommended that a series of parallel and impinging flow, forced convection calculations with various

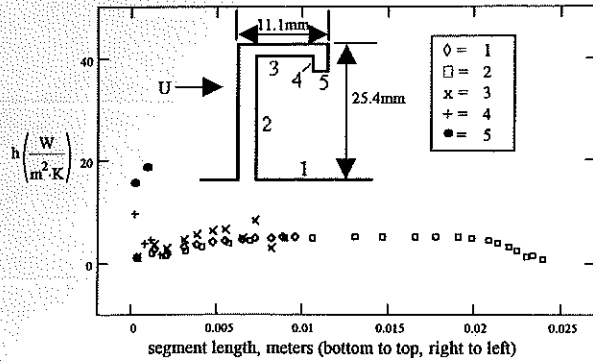


Figure 5a Local heat transfer coefficient on the sheltered surfaces of the frame from the "protrusion detail" calculations; upstream frame (sill).

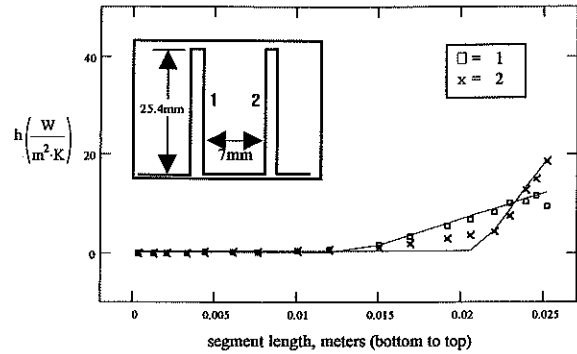


Figure 5b Local heat transfer coefficient on the sheltered surfaces of the frame from the "protrusion detail" calculations; downstream frame (head).

fenestration system geometries should be performed (similar to the current study) to develop standard heat transfer coefficient boundary condition correlations to use in two-dimensional conduction-only computer programs. The study should give results that are in nondimensional form so that they can be widely employed (e.g., local Nusselt number as a function of the local Reynolds number based on the window geometry and free-stream velocity).

ACKNOWLEDGMENTS

The authors would like to acknowledge the financial support of the Office of Building Systems of the United States Department of Energy under financial assistance award number DE-FG36-94CH10604. The authors would also like to acknowledge a supercomputer grant from the Energy Research Scientific Computing Center, which is supported by the Office of Energy Research of the United States Department of Energy. Without the above support, this research would not have been possible. Any opinions, findings, and conclusions or recommendations expressed in this paper are those of the authors and do not reflect the views of the above granting agencies.

NOMENCLATURE

Symbols

| | |
|-------------|--|
| c | = specific heat [energy/(mass·degree)] |
| h | = convective heat transfer coefficient [energy/(time·length ² ·degree)] |
| h_x | = local heat transfer coefficient [energy/(time·length ² ·degree)] |
| k | = specific turbulence kinetic energy [length ² /time ²] |
| L | = characteristic length [length] |
| P | = pressure [force/length ²] |
| T | = temperature [degree] |
| T_{fluid} | = fluid film temperature [degree] |

ΔT = characteristic temperature difference [degree]

u = x component of velocity [length/time]

U = characteristic velocity [length/time]

v = y component of velocity [length/time]

x, y = Cartesian coordinate directions [length]

NOTE: energy = force·length and force = mass·length/time²

Greek Letters

α = $\lambda/\rho \cdot c$ = thermal diffusivity [length²/time]

β = coefficient of thermal expansion [1/degree]

ϵ = dissipation of turbulence kinetic energy [length²/time³]

λ = thermal conductivity [energy/(time·length·degree)]

μ = dynamic viscosity [mass/(length·time)]

μ_t = eddy (turbulent) viscosity [mass/(length·time)]

ρ = density [mass/length³]

σ_ϵ = dissipation closure coefficient

σ_k = kinetic energy closure coefficient

τ_x = local wall shear stress [force/length²]

ν = μ/α = kinematic viscosity [length²/time]

Dimensionless Groups

Prandtl number: $Pr = \nu/\alpha$

Peclet number: $Pe = Re \cdot Pr = U \cdot L/\alpha$

Local Peclet number: $Pe_x = Re_x \cdot Pr = U \cdot x/\alpha$

Stanton number: $St = h/(\rho \cdot c \cdot U)$

Local Stanton number: $St_x = h_x/(\rho \cdot c \cdot U)$

Reynolds number: $Re = U \cdot L/\nu$

Local Reynolds number: $Re_x = U \cdot x/\nu$

Local skin friction coefficient: $C_{fx} = \tau_x / [(1/2) \cdot \rho \cdot U^2]$

Superscripts

\circ = nondimensional quantity

REFERENCES

- ASHRAE. 1996. ASHRAE Draft Standard 142P, Standard method for determining and expressing the heat transfer and total optical properties of fenestration products. Atlanta: American Society of Heating, Refrigerating and Air-Conditioning Engineers, Inc.
- ASHRAE. 1997. *1997 ASHRAE Handbook—Fundamentals*. Atlanta: American Society of Heating, Refrigerating and Air-Conditioning Engineers, Inc.
- Baker, A.J. 1983. *Finite element computational fluid mechanics*. Hemisphere.
- Branchaud, T.R. 1997. Two-dimensional finite element analysis of laminar and turbulent convective heat transfer over the exterior surface of a fenestration system. Master of science thesis, Mechanical Engineering Department, University of Massachusetts.
- Burnett, D.S. 1987. *Finite element analysis, from concepts to applications*. Addison Wesley.
- Curcija, D. 1992. Three-dimensional finite element model of overall, night time heat transfer through fenestration systems. Ph.D. thesis, Department of Mechanical Engineering, University of Massachusetts.
- Curcija, D., and W.P. Goss. 1993. Two-dimensional natural convection over the isothermal indoor fenestration surface—Finite element numerical solution. *ASHRAE Transactions* 99 (1): 274-287.
- Curcija, D., and W.P. Goss. 1994. Two-dimensional finite element model of heat transfer in complete fenestration systems. *ASHRAE Transactions* 100 (2): 1207-1221.
- Curcija, D., and W.P. Goss. 1995. Two-dimensional forced convection perpendicular to the outdoor fenestration surface—FEM solution. *ASHRAE Transactions* 101 (1): 201-209.
- FDI. 1993. *FIDAP user's manual*. Fluid Dynamics International, Evanston, IL.
- Holman, J.P. 1990. *Heat transfer*, 7th ed. McGraw-Hill.
- Launder, B.E., and D.B. Spalding. 1972. *Lectures in mathematical models of turbulence*, chapters 4 and 5. London and New York: Academic Press.
- ISO. 1998. prEN ISO/CD 10077, Part 2: Windows, doors and shutters—calculation of thermal transmittance; Part 2: Numerical method for frames. International Standards Organization committee draft.